Kinetics of dissolution and growth of calcium fluoride and effects of phosphate

Jørgen Christoffersen, Margaret R. Christoffersen, Wiktor Kibalczyc and W. G. Perdok

Department of Medical Chemistry, Panum Institute, University of Copenhagen, Copenhagen, Denmark; Institute of Physics, Technical University of Lódź, Lódź, Poland; and Laboratory for Materia Technica, State University of Groningen, Groningen, The Netherlands

Christoffersen J, Christoffersen MR, Kibalczyc W, Perdok WG. Kinetics of dissolution and growth of calcium fluoride and effects of phosphate. Acta Odontol Scand 1988;46:325–336. Oslo. ISSN 0001-6357.

The rate of growth of pure calcium fluoride crystals is controlled by a surface polynuclear mechanism when the supersaturation is less than 4.4. The surface free energy is found to be 120 mJ/m^2. The dissolution process is also controlled by a surface process. Both of these processes are very strongly inhibited by phosphate ions. Calcium fluoride-like materials contaminated with phosphate are formed when calcium fluoride is precipitated in phosphate-containing solutions or suspensions. The physical and chemical properties of these materials have been investigated and compared with the corresponding properties of pure calcium fluoride. The former dissolve much faster than pure calcium fluoride in solutions containing phosphate, but an inhibitory effect is still shown. It is suggested that the calcium fluoride-like material formed on dental enamel during treatment of enamel with acidified solutions of high fluoride content is a phosphate-containing calcium fluoride. □ *Apatites; dental deposits; dental enamel; dental enamel solubility; fluorides, topical*

Jørgen Christoffersen, Medicinsk-Kemisk Institut, Panum Instituttet, Blegdamsvej 3, DK-2200 Copenhagen N, Denmark

Calcium fluoride crystals have important industrial applications. These crystals, or crystals contaminated with phosphate, are also of interest in dentistry owing to their possible anti-caries effects. Despite the importance of these crystals, the mechanisms controlling the dissolution and growth processes appear not to be unambiguously known. This is also the case for the surface tension of the crystals in aqueous solution.

Gardner & Nancollas (1) studied the kinetics of both the growth and the dissolution processes at 25°C and found the rate of growth to be proportional to $(S-1)^n$, with S being the supersaturation ratio C/C_s. At low supersaturation, $S \leq 1.75$, the value of n was 3, and for $1.75 \leq S \leq 3$, the reported value of n is 2. The rate of dissolution was proportional to $(S-1)$, but with a rate constant too small for the rate of dissolution to be diffusion-controlled. Gardner & Nancollas (1) thus concluded that both processes were controlled by surface processes. Shyu & Nancollas (2) reported the rate of growth of calcium fluoride crystals at 37°C to be proportional to $(S-1)^2$ in the supersaturation range $1.2 \leq S \leq 2.66$. In these experiments a constant composition method was applied. Nielsen & Toft (3) studied the rate of growth of calcium fluoride at 25°C during direct crystallization and found the rate of growth to be controlled by a polynuclear mechanism, the rate being proportional to $(S-1)^n$ with $n>2$ in the supersaturation range $4 \leq S \leq 40$. At lower supersaturation, the rate was proportional to $(S-1)^2$.

The surface tension of crystals in aqueous solution greatly influences the rate at which processes can take place in the surface of the crystals. Nielsen & Söhnel (4) reviewed the literature and concluded the 'best value' for the surface tension of calcium fluoride to be $\sigma = 280$ mJ/m^2. de Jong et al. (5) used contact angle measurements and obtained a much lower value (≈ 40 mJ/m^2).

In dentistry topical application of fluoride-containing compounds normally causes precipitation of calcium fluoride or calcium fluoride-like material containing some

phosphate. Dental application of such agents is not unanimously accepted. The morphology and structure of such precipitates on enamel have recently been described in detail by Nelson et al. (6, 7). A generally accepted physical model describing the interaction between dental enamel and topically applied fluoride-rich agents has been given by Higuchi et al. (8). In this model, calcium fluoride precipitates on the enamel and, owing to ion exchange, a layer of calcium hydroxyapatite (HA) beneath the calcium fluoride layer may be transformed into fluorapatite (FA). From a dental point of view it is desirable to have HA in enamel transformed into FA, as the latter is more resistant to acid attack than HA. The price for this transformation, when topical fluoride-rich agents are applied, appears to be that the calcium ions precipitated originate from the enamel. McCann (9) has described the interaction between HA, FA, and CaF_2 in detail and reports that at low pH values calcium fluoride is less soluble than FA. If this were not the case, calcium fluoride-like material could not be formed on enamel during topical fluoride application. This means that a model assuming that calcium fluoride-like material precipitated on enamel can act as a desirable fluoride buffer may not be quite as acceptable as often considered. If acid can penetrate the calcium fluoride layer, FA may dissolve, and more calcium fluoride may be formed.

The rates of growth (2) and dissolution (10, 11) of calcium fluoride crystals are severely reduced if phosphate is present. This inhibitory effect decreases with decreasing values of pH (11). Lagerlöf et al. (11) report that, clinically, intermittent treatment with high concentrations of fluoride is an acknowledged caries-preventive measure. This statement is based on the concept that calcium fluoride inhibited by phosphate acts at low pH as a slow-release device for fluoride, which at higher pH can be reprecipitated as FA or adsorbed onto HA in the underlying enamel.

To help elucidate this subject, basic information concerning solubility and kinetics of growth and dissolution of pure calcium fluoride crystals and calcium fluoride-like crystals containing phosphate appears to be required, as does information about the multi-phase system consisting of HA, FA, CaF_2, and CaF_2-like crystals suspended in aqueous solution containing at least calcium, hydrogen or dihydrogen phosphate, and fluoride ions at various pH values.

The aims of the present work are to determine the rates of growth and dissolution of pure calcium fluoride in aqueous suspensions and possible mechanisms controlling these processes, and to study the properties of the calcium fluoride-like material formed by adding fluoride to systems containing HA crystals and/or dissolved calcium and phosphate, simulating the type of calcium fluoride-like material formed on dental enamel as a result of topical treatment with acidified solutions of high fluoride content.

Materials and methods

Stock crystals, formation, and characterization

All chemicals were of analytical grade. The pyrophosphate content of phosphate solutions was reduced by treatment with alkaline phosphatase (Boehringer Mannheim, 108146), the enzyme subsequently being removed by pressure-filtering through a Diaflo PM10 ultrafiltration membrane. Deionized water, further purified by a Millipore Milli-Q analytical water system, was used.

Pure CaF_2, called CaF_2-0, was prepared by mixing equal volumes of 0.02 M $CaCl_2$ and 0.04 M KF. The crystals were rinsed free of KCl and the suspension concentrated to approximately 100 mg/ml. These crystals, shown in Fig. 1a, are characterized as roughly cubic, approximately 1–2 μm in length, and their specific surface area is 1.4 m^2/g, determined by the single-point (30% nitrogen, 70% helium) BET method using a Quantasorb instrument.

Phosphate-contaminated CaF_2, type 1, called CaF_2(P)-1, was prepared by adding 5.0 ml 1 M KF to 1 l solution, approximately saturated with regard to HA at pH 5, containing 4.0 mmol $Ca(NO_3)_2$ and 2.4 mmol K-PO_4 buffer. The pH decreased to 4 on

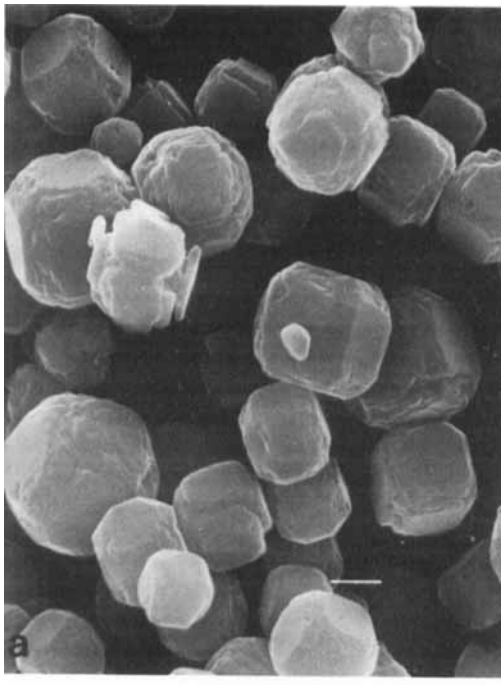

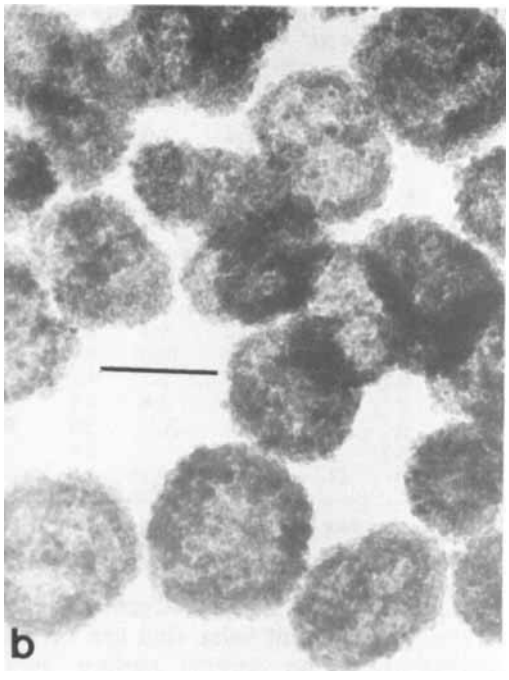

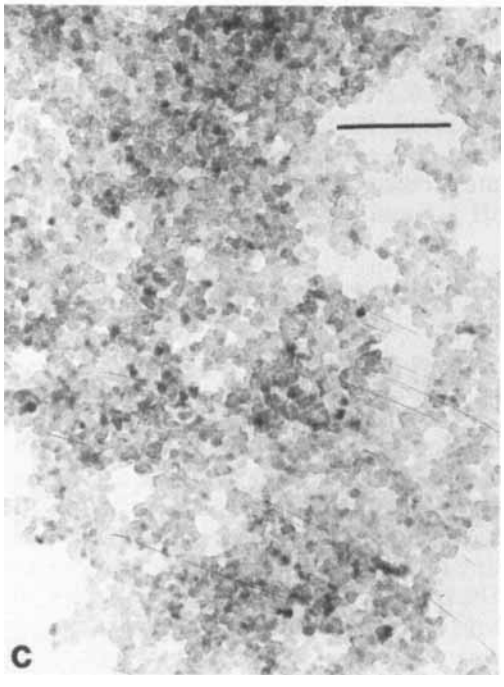

Fig. 1a. SEM photograph of CaF_2-0 stock crystals. The line in the figure represents 1 μm. 1b and c. TEM photographs of CaF_2(P)-1 and CaF_2(P)-2, respectively. The lines drawn in the figures represent 100 nm.

mixing. Further details are given in Table 1, experiment 3. The globular precipitate formed is shown in Fig. 1b. The agglomerates are characterized as roughly spherical, approximately 0.1 μm in diameter, with a specific surface area of 71 m^2/g. Assuming a spherical form and a density of 3.18 g/cm^3, the value of the surface area would indicate a diameter of 0.03 μm. We thus assume that the 'globules' are composed of many smaller crystals. The molar ratios of Ca/F and Ca/P are 0.55 and 10, respectively. The composition of these crystals can be expressed by the formula $CaF_{1.8}(HPO_4)_{0.1}$. The mass of these crystals, measured in a Mettler TA3000 thermal balance, decreased by 3.2% during heating from 100°C to 700°C, after being dried for 2 h at 100°C.

Phosphate-contaminated CaF_2, type 2, called CaF_2(P)-2, was prepared by adding 50 ml 1 M KF to 1 l metastable supersaturated solution of HA at pH 5.0, containing 40 mmol $Ca(NO_3)_2$ and 24 mmol K-PO_4 buffer. The pH decreased to 3.0 on mixing. Further details are given in Table 1, experiment 5. These crystals, shown in Fig. 1c, are characterized as roughly spherical

Table 1. Formation of calcium fluoride-like materials containing phosphate*

Expt.	*t*/h	[Ca]	[PO_4]	[F]	pH	m_{HA}
1	0	4.0	2.4	1.0	5.0	175
	0.1			0.6	4.2	
	2	3.7	2.3	0.6	4.0	
2	0	4.0	2.4	1.0	5.0	0
	0.1				4.8	
	20	3.7	2.36	0.4	4.5	
3	0	4.0	2.4	5.0	4.8	0
	0.1			0.7	3.8	
	100	1.4	2.2	0.4	3.8	
4	0	4.0	2.4	10.0	5.0	175
	0.1			2.7	4.2	
	2	0.09	2.6	2.6	4.9	
5	0	40	24	50	5.0	0
	0.1				3.0	
	100	11	21	0.15	3.0	

* Concentrations in mmol/l; mass in mg/l.

and approximately 0.01–0.02 μm in diameter, which is about value that can be calculated from the specific surface area, 123 m^2/g. The molar ratios Ca/F and Ca/P are 0.58 and 5.3, respectively. The composition of these crystals can be expressed by the formula $CaF_{1.7}$ $(HPO_4)_{0.1}(H_2PO_4)_{0.1}$. The mass of these crystals decreased by 4.3% during heating from 100°C to 700°C, after being dried for 2 h at 100°C.

The CaF_2(P)-1 and CaF_2(P)−2 crystals were further studied and compared with CaF_2-0 and a pure natural sample of fluorite by roentgenography, electron diffraction, and IR spectrometric techniques.

Kinetics of dissolution of pure calcium fluoride

All experiments were carried out at 25°C in an atmosphere of nitrogen. A portion of stock crystals of CaF_2-0 in suspension form was added to an undersaturated solution, the composition of which was kept constant by using the signal from either a conductivity meter or an electrochemical cell to control a pH-stat regulating the addition of water from a burette. Radiometer's conductivity cell PP1042, conductivity meter CDM3, fluoride electrode F1052F, calomel electrode K102, and pH-stat equipment were used. Experiments were carried out in the saturation ratio range $0.2 \leq C/C_s \leq 0.75$, where C is the stoichiometric concentration of CaF_2 kept constant and C_s is the solubility concentration. Stock crystals, 9–34 mg, were added to 600 ml solution and titrated with approximately 400 ml water. Calcium concentrations, measured by means of a Perkin-Elmer 4000 atomic absorption spectrometer, of the initial solution, the filtrate after an experiment, and the final acidified reaction mixture were used to check the constancy of the concentration and to calculate the initial mass of stock crystals added.

Care was taken to ensure that the signal at a given composition was independent of the volume in the reaction vessel. As a further check, some experiments were made at constant volume by adding stock crystals to water and following either the change in fluoride concentration by electrode measurements or the change in conductance.

The effect of phosphate on the rate of dissolution was studied by adding 0.5 μmol phosphate solution to 1 l reaction mixture in which approximately 23 mg CaF_2-0 was dissolved in water at a saturation ratio of about 0.2. Calcium concentrations were measured in filtered samples taken just before the addition of phosphate and at two later times. This effect was studied at pH 3, 4, and 5.

Kinetics of crystal growth of pure calcium fluoride

These experiments were made at 25.0°C by seeding a supersaturated solution with CaF_2-0 crystals and keeping the concentrations constant. The supersaturated solutions were prepared by adding equal volumes of 10^{-2} M $Ca(NO_3)_2$ and 2×10^{-2} M KF from Radiometer ABU80 burettes to 700 ml 10^{-2} M KNO_3 solution in a reaction vessel. The composition of the reaction solution was kept constant throughout an experiment by means of Radiometer pH-stat equipment, in which the two burettes were coupled by means of a Radiometer Burette synchronizer, which ensured that equal volumes from the two burettes were always added to the reaction mixture. The fluoride and reference electrodes specified in the previous section

were used to control the pH-stat. The experiments were made in an atmosphere of nitrogen. Crystals, 19–36 mg in suspension form, were used in experiments, and the saturation ratio studied was in the range $2 \leq C/C_s \leq 4.4$. The constancy of the calcium concentration was checked, and the initial mass of crystals was determined by acidifying the final reaction mixture and measuring the total calcium content.

The effect of phosphate on the rate of growth was investigated by adding 0.02–0.2 μM phosphate to the supersaturated solution before the addition of crystals.

Reactions between calcium, phosphate, and fluoride ions and HA

Potassium fluoride was added to 40 ml solution approximately saturated at pH 5.0 with regard to HA (4 mM $Ca(NO_3)_2$ and 2.4 mM K-PO_4), containing 7 mg HA, to make a total concentration of 1 mM KF or 10 mM KF. The pH and the fluoride concentration were measured over time, and the calcium and phosphate concentrations in filtered samples removed after 2 h were measured. Electron micrographs were taken at various times during the reaction. The experiment with 1 mM KF was repeated without HA. In this case the fluoride, calcium, and phosphate concentrations in solution were measured after 20 h. Details of two further experiments, the preparations of CaF_2(P)-1 and CaF_2(P)-2 have been given in a previous section.

Electron and X-ray diffraction

Electron diffraction patterns were determined by means of a Carl Zeiss EM109 electron microscope at 80 kV. A sample of pure natural fluorite was used as standard.

For the X-ray diffraction investigations a Philips diffractometer was used, the X-ray tube having a copper anode with nickel filter (Cu Kα radiation). For the determination of the lattice parameter of CaF_2-0 a very pure silicon standard was applied in the form of a flat slice of pressed silicon powder, provided with two shallow rectangular cavities into which the finely powdered sample was pressed with a glass slide, so that its flat surface coincided with the surface of the silicon slice. The quality of crystallization of CaF_2(P)-1 and CaF_2(P)-2 was such that the silicon standard could not be used, as the broad reflections of the calcium fluoride samples overlapped the sharp silicon standard lines. Therefore the values of the lattice parameters of CaF_2(P)-1 and CaF_2(P)-2 are less accurate than that of CaF_2-0.

Solubility and dissolution rate of phosphate-incorporated calcium fluoride

Approximately 30 mg CaF_2(P)-1 was added to 900 ml water, and approximately 30 mg CaF_2(P)-2 was added to 900 ml water and to 900 ml 2 mM phosphate buffer, pH 6 (simulating saliva conditions). The change in fluoride concentration with time was measured by means of fluoride–calomel electrode measurements. The calcium concentration in filtered samples was also measured. Similar experiments with CaF_2-0 were done for comparison, but here the phosphate concentration was 1 μM.

Results

Kinetics

The rate, J, of crystal growth and dissolution for seeded experiments can (12, 13) be expressed by

$$J \equiv |dn_{cr}/dt| = K' m_o F(m/m_o) g(C) \quad (1)$$

in which J is the rate, n_{cr} is the amount of substance in the crystals, t is time, K' is a rate constant, m_o is the initial mass of crystals, m is the actual mass of crystals at time t, $F(m/m_o)$ is a term representing the influence of crystal morphology, size, and so forth on the rate, and $g(C)$ is a function representing the influence of the solution composition on the rate. In this work results of dissolution and growth experiments are reported only for $m/m_o = 0.9$ and $m/m_o = 2$, respectively. In both cases the term $F(m/m_o)$ is a constant and can be included in the rate constant, $K = K'F(m/m_o)$.

For diffusion-controlled growth or dis-

solution, the rate can be expressed as

$$J = m_o DA(C_s - C)/\delta \qquad (2)$$

in which D is the diffusion coefficient, A the area of the crystals, normally increasing with m/m_o, and δ is the thickness of the diffusion layer, here estimated to be of the order 1 μm. For very small crystals, δ should be replaced by the linear dimension of the crystals.

For spiral growth and dissolution, the rate is normally proportional to $(C_s - C)^p$ with p close to 2. The spiral growth or dissolution mechanism seems not to apply to CaF_2. Rate expressions for these mechanisms have recently been discussed (14, 15).

If the rate of crystal growth is controlled by small nuclei (islands) being formed on flat crystal surfaces, and if these nuclei intergrow, the rate is said to be controlled by a polynuclear mechanism. In this case, the concentration term, $g(C)$, in eqn. (1) can be expressed (13) as

$$\begin{aligned} g(C) &= C^{1/3}(S-1)^{2/3}\beta^{1/6}\exp(-\alpha/\beta) \\ &= f(C)\exp(-\alpha/\beta), \end{aligned} \qquad (3)$$

in which S is the supersaturation ratio C/C_s and β is the growth affinity, $\beta = \ln(Y/K_s)^{1/\nu}$, Y being the ion activity product, K_s the solubility product, and ν the number of ions in a formula unit. $\beta \approx \ln S$ for stoichiometric solutions. α is given by

$$\alpha = \pi a^4 \sigma^2/3(kT)^2, \qquad (4)$$

in which a is an average ion size, σ is the surface energy, and kT is the Boltzmann constant times the (Kelvin) temperature. For constant values of m/m_o a plot of $\ln(J/m_o f(C))$ against $-1/\beta$ should give a straight line if the rate of growth is controlled by this mechanism.

Dissolution

Results of dissolution experiments are given in Fig. 2, in which log-(J/m_o) is plotted against $\log(1 - S)$. A single experiment contributes only one point to this plot. The solubility product was taken to be 2.3×10^{-11} M^3, from which the solubility in water is 0.19 mM. The slope of the line drawn is 0.8 ± 0.2. (Using the value

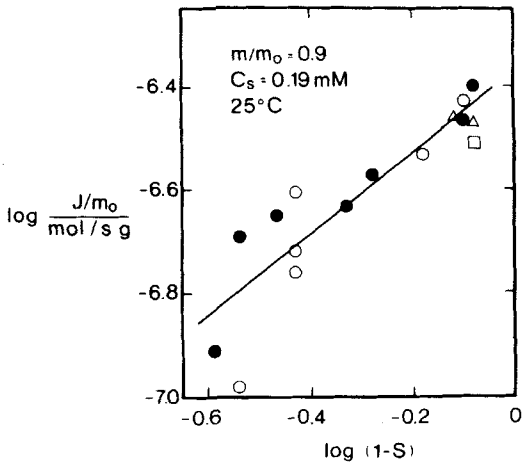

Fig. 2. Logarithmic plot of the rate, J/m_o, as a function of $(1 - S)$ for the dissolution of CaF_2-0 in aqueous solution. (●, ○) Constant composition experiments with (●) fluoride electrode or (○) conductance control. (□, △) Constant volume experiments with (□) fluoride electrode or (△) conductance measurement. The rate is measured in each experiment when 10% of the initial mass of crystals is dissolved.

2.8×10^{-11} M^3 for the solubility product (1) and thus 0.20 mM for the solubility leads to a slope of 0.85.) This could indicate that the rate is diffusion-controlled, in which case the slope of the line should be 1. However, the rate constant obtained by extrapolation of the line to $S = 0$ is too small to account for the rate being diffusion-controlled. From the rate constant an apparent value of the diffusion coefficient, D_{ap}, can be obtained from

$$D_{ap} = K\delta/C_s A_{sp} \approx 2 \times 10^{-8} \text{ cm}^2/\text{sec}, \qquad (5)$$

in which A_{sp} is the specific surface area, C_s is the saturation concentration, taken to be 0.19 mM, and δ is the thickness of the diffusion layer, here assumed to be 1 μm. Diffusion coefficients are normally of the order of 10^{-5} cm^2/sec. A similar result was obtained by Gardner & Nancollas (1). From these results we may, as they did, conclude that the rate of dissolution of pure calcium fluoride is controlled by a surface process, although such processes are normally expected to give a higher slope than 1 in a plot of the type shown in Fig. 2.

Phosphate-induced inhibition of dissolution of pure calcium fluoride crystals is a

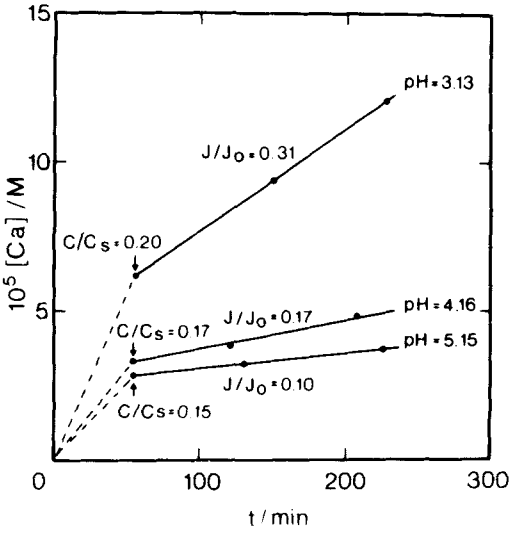

Fig. 3. Calcium ion concentrations in solution as a function of time during experiments in which 23 ± 1 mg CaF_2-0 is dissolved at constant pH in 1 l dilute HNO_3 solution with the addition of 0.5 μmol phosphate (pH adjusted) buffer at the time shown by arrows. 25°C.

well-established phenomenon (10, 11). This effect is also shown in Fig. 3, in which the calcium ion concentration for experiments in which crystals were added to water with pH adjusted to 3.13, 4.16, and 5.15 is plotted against time. At time $t = 55$ min, phosphate buffer was added to give a total phosphate concentration of 0.5 μM. The calcium ion concentrations in the time interval 0 to 55 min are approximated by the stippled lines. The rates of dissolution were determined just before, J_o, and just after, J, the addition of phosphate. The ratio J/J_o is also given on the plot. From this plot it can be seen that the inhibitory effect of phosphate decreases with decreasing values of pH, as found by Lageröf et al. (11). The effect of inhibitors for crystal growth and dissolution processes normally increases as saturation is approached (16). Since the ratio J/J_o takes the pH dependence of the rate of dissolution of calcium fluoride into account, and as the degree of saturation at the time the phosphate was added increases with decreasing pH, we can conclude that the pH dependence of J/J_o can be a result of changes in the ion speciation of phosphates, in agreement with the conclusion drawn by Chander et al. from electrophoretic studies (17). Nothing, however, can be concluded from Fig. 3 about how phosphate will interfere with dissolution of calcium fluoride-like material containing some phosphate.

Growth kinetics

Results of growth kinetic experiments are given in Fig. 4, in which $\log(J/m_o)$ is plotted against $\log(S - 1)$ (see eqn. (1)). In this plot all points originate from separate experiments. The rates were determined at times when the crystals had grown to double their original mass. When the value 0.22 mM is used for the solubility, calculated from the solubility product 2.3×10^{-11} M^3, with the ionic strength of the solvent being 0.01 M, the slope of the line is, as drawn, 3.0 ± 0.1. (The value 0.24 mM for the solubility, from the solubility product 2.8×10^{-11} M^3, leads

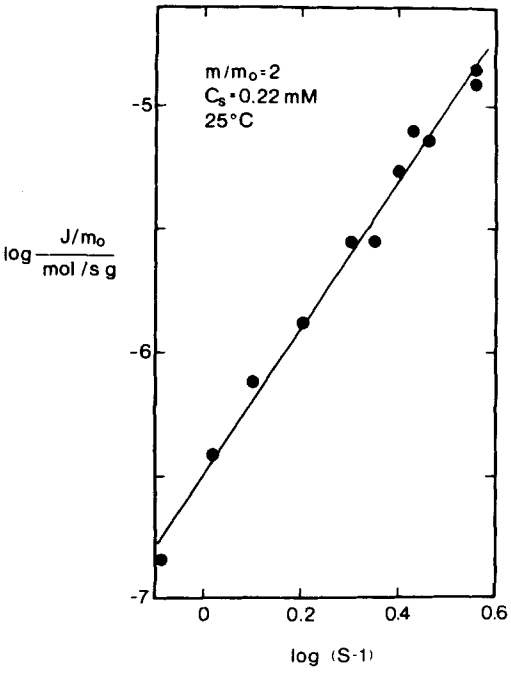

Fig. 4. Logarithmic plot of the rate, J/m_o, as a function of $(S - 1)$ for growth of CaF_2-0 in supersaturated solutions with concentrations held constant by fluoride electrode control. The rate is measured in each experiment at the time when the crystals have doubled their original mass.

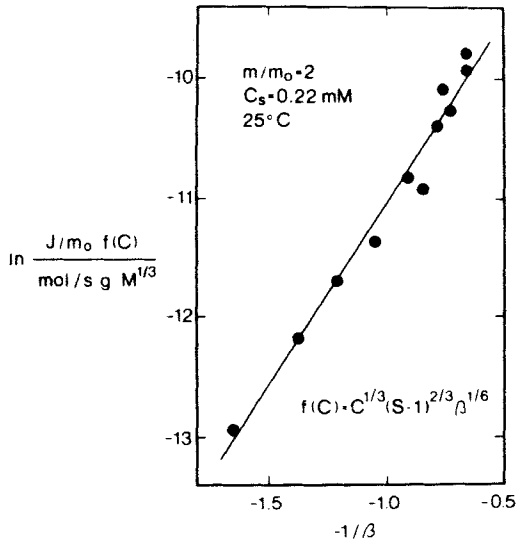

Fig. 5. The results shown in Fig. 4 plotted in accordance with the polynuclear mechanism of crystal growth. From the slope of the line, 3, a value for the surface free energy of 120 mJ/m^2 can be calculated.

to a line with a slope of 2.8.) This indicates that the rate of growth of pure calcium fluoride crystals is controlled by a surface process other than a spiral mechanism. The results given in Fig. 4 are replotted in Fig. 5 in accordance with an expression for a polynuclear mechanism; see eqns. (1, 3). As a straight line is obtained, we can conclude that the rate of growth of pure calcium fluoride crystals can be described by the polynuclear mechanism being rate-controlling. From the slope of the line in Fig. 5 the value of the surface free energy, $\sigma = 120$ mJ/m^2, can be calculated using eqn. (4) and assuming a mean ion size of 2.4 Å.

We found 0.16 μmol phosphate to be sufficient to inhibit severely the growth of 25 mg CaF_2-0 in 800 ml supersaturated solution with $S = 3.5$, pH ≈ 7, in agreement with earlier reported results (2).

Formation of calcium fluoride-like materials containing phosphate

In Table I results are given for experiments in which sodium fluoride solution was added to calcium- and phosphate-containing solutions, some of which also contained HA. The solutions produced were all supersaturated with regard to calcium fluoride and FA. In experiments 1–4 the solution was saturated with regard to HA. In experiment 1 no calcium fluoride material could be detected in transmission electron micrography (TEM) studies. The decrease in pH is apparently caused by growth of FA on the apatite crystals. In experiment 2, which is identical to experiment 1 except that HA was not present, calcium fluoride material could be detected after about 20 h. In experiment 3, in which the initial fluoride concentration was higher than in experiments 1 and 2, calcium fluoride-like material was precipitated quickly. The precipitate is that described in the first section in Materials and methods and called CaF_2(P)-1. An electron micrograph is given in Fig. 1b. The precipitate was not pure calcium fluoride,

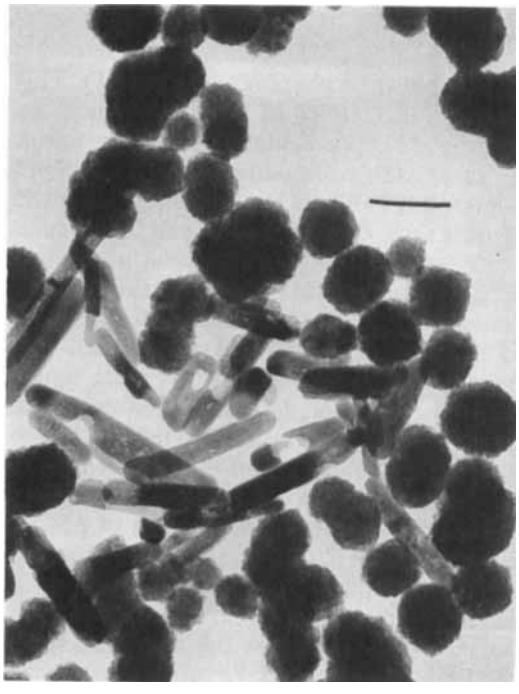

Fig. 6. TEM photograph of the crystals present in experiment 4, Table 1, 1 h after mixing. In connection with the precipitation of CaF_2-like material, lack of calcium ions in solution as compared with the fluoride ion concentration causes calcium ions to be provided by HA crystals, resulting in partial dissolution of HA. The line drawn in the figure represents 100 nm.

but a calcium fluoride-like material with Ca/P ≈ 10. In experiment 4, in which the fluoride concentration was further increased and HA was present, calcium fluoride-like material precipitated and HA crystals partially dissolved (Fig. 6). Increasing the fluoride concentration to 50 μM caused complete dissolution of the HA. In experiment 5, in which calcium, phosphate, and fluoride concentrations were higher than in experiment 3 by a factor of 10, a very fine precipitate of calcium fluoride-like material with Ca/P ≈ 5 was produced. This precipitate was also described in the first section of Materials and methods and called CaF_2(P)-2.

Infrared spectra and electron and X-ray diffraction of calcium fluoride and calcium fluoride-like materials

The infrared spectra of CaF_2(P)-1 and CaF_2(P)-2 are very similar and clearly show the presence of phosphate around 1100 cm^{-1}, an absorption that is completely lacking in the infrared spectrum of CaF_2-0.

CaF_2(P)-1 and CaF_2(P)-2 give surprisingly sharp electron diffraction patterns, which are very similar to the electron diffraction pattern of pure calcium fluoride. The electron diffractogram of CaF_2(P)-2 is shown in Fig. 7. In Fig. 7, 1.0 cm represents 1.0 cm. The *d* spacings can be calculated from

$$d/\text{Å} = 3.2758/(D/\text{cm}), \qquad (6)$$

which was determined from the electron diffraction pattern of pure calcium fluoride, photographed under the same conditions. *D* is a ring diameter. The *d* spacings calculated from electron diffraction patterns of CaF_2(P)-1, CaF_2(P)-2, and the X-ray diffraction values of *d* for pure CaF_2 (18) are given in Table 2. The electron diffraction pattern of calcium fluoride-like material deposited by fluoride treatment of enamel has been shown to resemble that of pure calcium fluoride (7).

The results of X-ray diffraction investigations are given in Table 3 as lattice parameter values for the cubic lattice. CaF_2-0 was found to be very well crystallized. The lattice parameter is slightly larger than that of other pure samples of CaF_2. This may indicate that CaF_2-0 contains traces of chloride. CaF_2(P)-1 and Ca_2(P)-2 are less well crystallized, showing broader and less intense reflections than CaF_2-0. The lattice parameters of CaF_2(P)-1 and CaF_2(P)-2 are less accurately determined but very similar to that of CaF_2-0.

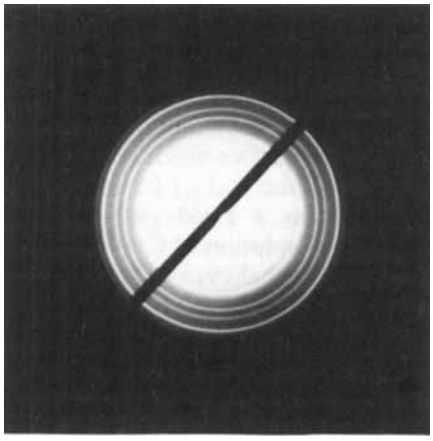

Fig. 7. Electron diffraction pattern of CaF_2(P)-2. In this figure 1.0 cm represents 1.0 cm, and the d spacings can be calculated from eqn. (6).

Table 2. d-spacings from electron diffraction patterns of CaF_2(P)-1 and CaF_2(P)-2 and from X-ray diffraction measurements for pure CaF_2 (18). d is given in Å

CaF_2(P)-1	CaF_2(P)-2	CaF_2 (pure)
3.03 vs	3.12 vs	3.155 vs
2.73	2.75	2.7314
1.92 vs	1.92 vs	1.9316 vs
1.60 vs	1.64 vs	1.6471 vs
1.56	1.56	1.5771
1.36	1.37	1.3656
1.25	1.25	1.2533
		1.2216 vw
1.11	1.10	1.1152
1.05	1.04	1.0514
0.96	0.96	0.9658
0.92	0.92	0.9234
		0.9105 vw
0.86	0.87	0.8638
0.84	0.84	0.8331
0.79	0.80	0.8236

Table 3. The lattice parameter a for samples of CaF_2 and CaF_2-like materials calculated from X-ray diffraction

CaF_2 (18)	5.46305(8) Å
Fluorite mineral	5.4635 Å ± 0.0002 Å
Fluorite synthesized from melt	5.4626 Å ± 0.0002 Å
Fluorite suprapur	5.4624 Å ± 0.0002 Å
CaF_2-0	5.4657 Å ± 0.0002 Å
CaF_2-1	5.46 Å ± 0.01 Å
CaF_2-2	5.47 Å ± 0.01 Å

It thus seems difficult to find a quantitative difference between pure calcium fluoride and phosphate-containing calcium fluoride-like materials from electron or X-ray diffraction, the only difference appearing to be the broadening of the X-ray diffraction peaks.

Rate of dissolution of calcium fluoride-like materials

Results of experiments in which approximately 26 mg CaF_2, CaF_2(P)-1, or CaF_2(P)-2 dissolved in 0.9 l water or in phosphate buffer with pH ≈ 6 are shown in Fig. 8. In these experiments the release of fluoride was monitored. From this plot it can be concluded that both CaF_2(P)-1 and -2 crystals initially dissolve faster than pure CaF_2 crystals, for equal masses. The profiles of the dissolution curves for the calcium fluoride-like crystals are markedly different from that for the pure CaF_2 crystals. For pure CaF_2 the amount of fluoride released varies nearly linearly with time. For the CaF_2-like crystals, the rate of fluoride release is initially very fast but levels off. The initial rates for all three types of crystals are comparable, if the differences in the specific surface areas are taken into account. From these we would expect the rate of dissolution of CaF_2(P)-2 to be of the order 100 times, and that of CaF_2(P)-1 50 times the rate of dissolution of CaF_2-0 for equal masses, and this is approximately the case initially.

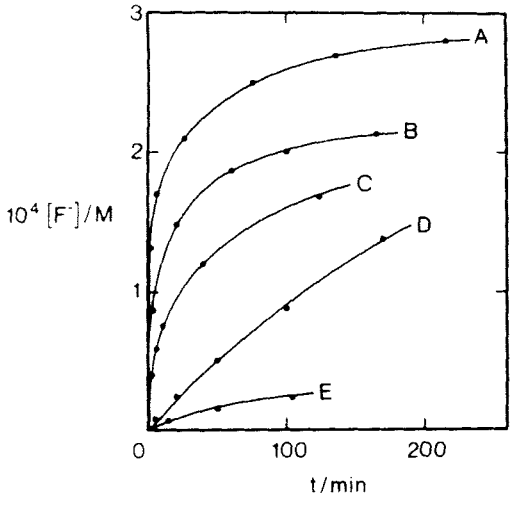

Fig. 8. Fluoride ion concentration plotted as a function of time for the dissolution of CaF_2-like materials and pure CaF_2 in water and in phosphate buffers. A = 28 mg CaF_2(P)-2 dissolved in water; B = 30 mg CaF_2(P)-1 in water; C = 28 mg CaF_2(P)-2 in 2 mM phosphate buffer; D = 23 mg CaF_2-0 in water; E = 25 mg CaF_2-0 in 1 μM phosphate buffer. pH ≈ 6; volume = 900 ml; 25°C in each case.

From Fig. 8 it can also be seen that the strong inhibitory effect of phosphate on dissolution of pure CaF_2 crystals is greatly reduced for CaF_2(P)-2. When the specific surface areas are taken into account, a 100-μM phosphate buffer should at least inhibit dissolution of the CaF_2(P)-2 crystals to the same extent as a 1-μM phosphate buffer inhibits the dissolution of CaF_2-0. From Fig. 8 it can be seen that even a 2-mM phosphate buffer does not inhibit CaF_2(P)-2 dissolution to this extent.

The smallest value for the ionic product $(Ca^{2+})(F^-)^2$ we have measured from precipitation of calcium fluoride containing phosphate is 12×10^{-11} M^3 (experiment 3, Table 1). The greatest value of the ionic product we have measured from dissolution experiments

with this material is 10×10^{-11} M^3. These values indicate a solubility of 0.33 mM in water, assuming the formula unit to be CaF_2, or 70% greater than the solubility of pure CaF_2.

Discussion

The results of seeded growth experiments with pure calcium fluoride crystals show that the rate of growth can be explained as controlled by the polynuclear mechanism in the supersaturation range $2 \leq S \leq 4.4$. This is in contradiction to the results reported in Refs. 1 and 2 but in agreement with results for $S > 4$ in Ref. 3. Rate constants, K_r, for the linear rate of growth, can be calculated (3) when the surface area of the crystals is known. In the present case,

$$K_r = KM/\rho A_s(m/m_o)^{2/3} = 4 \text{ pm/sec}, \quad (7)$$

where M is the molar mass and ρ is the density of the crystals. The value 5 pm/sec was reported (3) for calcium fluoride growing in solutions of low supersaturation, and the value 13 pm/sec can be calculated for results of growth experiments at 37°C (2).

The value obtained for the surface tension (Gibbs surface energy) $\sigma = 120 \text{ mJ/m}^2$ is smaller than the values discussed in Ref. 4 but greater than that reported for the (111) plane in Ref. 5. The value obtained in this work agrees well with that predicted from the plot of surface tensions against solubilities in Ref. 4.

The kinetic results for dissolution of pure calcium fluoride crystals are not simple to understand. The rate is proportional to $(S-1)^p$, with p close to 1, but the rate constant is too small for diffusion to be the rate-controlling mechanism. This result is in agreement with the results reported in Ref. 1. In Fig. 8 it can be seen that the rate of release of fluoride ions is practically linear with time in the initial part of the dissolution process. This could indicate that the following mechanism is important. Partial hydration of calcium ions situated in the crystal surface may cause bonds to fluoride ions to be weakened, corresponding to the fact that hydrated calcium ions do not form strong ion pairs in solution (their ion association constant being about 10). When fluoride ions leave the surface, because the neighbouring calcium ions have been partially hydrated, steric effects due to further hydration of surface calcium ions may hinder fast return of fluoride ions. As the surface tension is relatively high, the density of kink sites or dissolution holes (nuclei) is not expected to be very high, nor the surface to be naturally rough, and so we see no other mechanism that can explain the observed rate of dissolution than that outlined above.

McCann (9) showed that at low pH calcium fluorides are less soluble than FA. This is also the case for calcium fluoride material containing phosphate and is most important for the formation of calcium fluorides on dental enamel as a result of topical application of acidified agent with a high concentration of fluoride. The rate of fluoride release from such materials is much higher in phosphate-containing solutions than is the case for pure calcium fluoride, although less than the rate of dissolution in water.

To describe the inhibitory effect of phosphate on dissolution of pure calcium fluoride crystals, the following factors are most essential: density of crystals in suspension (g/l), concentration of phosphate adsorbed onto the crystal surfaces (mol/m^2), concentration of phosphate in solution, pH, and the degree of saturation with regard to calcium fluoride. The greater the total surface area of crystals in suspension, the larger the fraction of inhibitor adsorbed onto the crystal surface and the lower the concentration of inhibitor remaining in solution. From our results of dissolution of pure CaF_2 in systems containing phosphate it can be seen that 1 μM phosphate has a dramatic effect on the rate of dissolution of CaF_2. Dissolution rates determined (11) in a system containing 1 g/l CaF_2, with unknown specific surface area, in an aqueous solution containing 10 μM phosphate at pH 4 clearly show, when Figs. 4 and 2 (11) are compared, that also in this relatively dense system phosphate severely inhibits dissolution of CaF_2. Such results do not indicate that pure CaF_2 crystals precipitated on dental enamel could act as a

slow fluoride release device. The calcium fluoride-like materials containing phosphate appear to be more likely candidates to serve this purpose.

Acknowledgements.—J. Christoffersen and M. R. Christoffersen thank the Danish Medical Research Council, the Carlsberg Foundation, and Novo's Foundation for grants for laboratory assistance, equipment and travel. We are grateful to the Danish Natural Science Research Council for a study grant to W. Kibalczyc.

References

1. Gardner GL, Nancollas GH. Kinetics of crystal growth and dissolution of calcium and magnesium fluoride. J Dent Res 1976;55:342–52.
2. Shyu LJ, Nancollas GH. The kinetics of crystallization of calcium fluoride. A new constant composition method. Croatica Chem Acta 1980;53: 281–9.
3. Nielsen AE, Toft JM. Electrolyte crystal growth kinetics. J Crystal Growth 1984;67:278–88.
4. Nielsen AE, Söhnel O. Interfacial tensions electrolyte crystal-aqueous solution, from nucleation data. J Crystal Growth 1971;11:233–42.
5. de Jong HP, van Pelt HJ, Busscher HJ, Arends J. The surface tensions γ_s^p and γ_s^d of enamel, and of single crystals of biological interest. In: Frank RM, Leach SA, eds. Surface and colloid phenomena in the oral cavity. London: IRL Press Ltd., 1982;105–10.
6. Nelson DGA, Jongebloed WL, Arends J. Morphology of enamel surfaces treated with topical fluoride agents: SEM considerations. J Dent Res 1983;62:1201–8.
7. Nelson DGA, Jongebloed WL, Arends J. Crystallographic structure of enamel surfaces treated with topical fluoride agents: TEM and XRD considerations. J Dent Res 1984;63:6–12.
8. Higuchi WI, Valvani SC, Hefferren JJ. The kinetics and mechanisms of reactions of human tooth enamel in buffered solutions of high fluoride concentrations. Arch Oral Biol 1974;19:737–46.
9. McCann HG. The solubility of fluorapatite and its relationship to that of calcium fluoride. Arch Oral Biol 1968;13:987–1001.
10. Kanaya Y, Spooner P, Fox JL, Higuchi WI, Muhammad NA. Int J Pharm 1983;16:171–9.
11. Lagerlöf F, Saxegaard E, Barkvoll P, Rølla G. Effects of inorganic orthophosphate and pyrophosphate on dissolution of calcium fluoride in water. J Dent Res 1988;67:447–9.
12. Christoffersen J, Christoffersen MR. The kinetics of dissolution of calcium sulphate dihydrate in water. J Crystal Growth 1976;35:79–88.
13. Christoffersen J. Kinetics of dissolution of calcium hydroxyapatite. III. Nucleation-controlled dissolution of a polydisperse sample of crystals. J Crystal Growth 1980;49:29–44.
14. Christoffersen J, Christoffersen MR. Spiral growth and dissolution models with rate constants related to the frequency of partial dehydration of cations and to the surface tension. J Crystal Growth 1988;87:41–50.
15. Christoffersen MR, Christoffersen J. The kinetics of crystal growth and dissolution of calcium monohydrogen phosphate dihydrate. J Crystal Growth 1988;87:51–61.
16. Christoffersen J, Christoffersen MR, Christensen SB, Nancollas GH. Kinetics of dissolution of calcium hydroxyapatite. VI. The effects of adsorption of methylene diphosphonate, stannous ions and partly-peptized collagen. J Crystal Growth 1983; 62:254–64.
17. Chander S, Chiao CC, Fuerstenau DW. Transformation of calcium fluoride for caries prevention. J Dent Res 1982;61:403–7.
18. Mineral powder diffraction file data book. Swarthmore, Pa., USA: International Centre for Diffraction Data, 1986.

Received for publication 1 June 1988